International Journal of Nanomedicine

Dovepress
open access to scientific and medical research

Open Access Full Text Article

ORIGINAL RESEARCH

Gd^{3+}-DTPA-DG: novel nanosized dual anticancer and molecular imaging agent

This article was published in the following Dove Press journal:
International Journal of Nanomedicine
8 April 2011
Number of times this article has been viewed

Massoud Amanlou[1]
Seyed Davar Siadat[4,5]
Seyed Esmaeil Sadat Ebrahimi[1]
Abass Alavi[7]
Mohammad Reza Aghasadeghi[2]
Mehdi Shafiee Ardestani[1,4,6*]
Saeed Shanehsaz[2]
Masoud Ghorbani[6]
Bita Mehravi[8]
Mohammad Shafiee Alavidjeh[3]
Ali Jabbari-Arabzadeh[1]
Mehdi Abbasi[4]

[1]Department of Medicinal Chemistry, Faculty of Pharmacy; [2]Department of Medical Physics, School of Medicine; [3]Department of Pharmaceutics, Faculty of Pharmacy, Tehran University of Medical Sciences, Tehran, Iran; [4]Department of Hepatitis and AIDS; [5]Department of Microbiology; [6]R&D & QC & Hepatitis B & Nanobiotechnology Department, Research and Production Complex, Pasteur Institute of Iran, Tehran, Iran; [7]Department of Radiology, Division of Nuclear Medicine, School of Medicine, Pennsylvania University of Medical Sciences, Philadelphia, PA, USA; [8]Department of Nanomedicine, Shahid Beheshti Medical University, Tehran, Iran

Correspondence: Mehdi Shafiee Ardestani
Department of Nanobiotechnology, Hepatitis and AIDS, Pasteur Institute of Iran, Tehran, Iran
Tel/Fax +98 021 6695 3311
Email shafieeardestani@gmail.com

Background: Difficulties in the use, preparation, and cost of radioactively-labeled glycosylated compounds led to this research and development study of a new gadolinium-labeled glucose compound that does not have a radioactive half-life or difficulties in its synthesis and utilization.

Methods: Based on the structure of the 2-fluoro-2-deoxy-D-glucose molecule (^{18}FDG), a new compound consisting of D-glucose (1.1 nm) conjugated to a well-known chelator, diethylenetriamine penta-acetic acid (DTPA), was synthesized, labeled with Gd^{3+}, and examined in vitro and in vivo.

Results: This novel compound not only demonstrated excellent and less costly imaging capability, but also showed anticancer effects on treated cells. Our results demonstrated that the new Gd^{3+}-DTPA-DG compound (GDD, with GDD conjugate aggregation of about 8 nm at 0.02 mg/mL concentration) significantly decreased HT1080 and HT29 tumor cell numbers. Application of GDD to cancer cells also increased levels of tumor necrosis factor alpha, but did not alter blood glucose levels. Interestingly, no toxicological findings were seen in normal human kidney cells.

Conclusion: Dual application of GDD for both imaging and treatment of tumor cells could be remarkably advantageous in both the diagnosis and treatment of cancer.

Keywords: fluorodeoxyglucose, Gd^{3+}-DTPA-DG, positron emission tomography, diagnostics, treatment

Introduction

Cancer is a class of diseases in which groups of cells display uncontrolled growth (division beyond normal limits), invasion (intrusion on, and destruction of, adjacent tissues), and sometimes metastasis (spreading to other locations in the body via the lymph system or blood). These three destructive properties of cancerous tumors differentiate them from benign tumors, which are self-limiting, and do not invade or metastasize. Many cancers form a solid tumor but some, like leukemia, do not. Cancer affects people of all ages and was the cause of about 13% of all human deaths in 2007.[1] Cancers are caused by abnormalities in the genetic material of transformed cells.[1–3] They may be difficult to detect, but for some types of cancer, the earlier they are detected, the better the chances of effective treatment. Imaging techniques have become important in the early detection of many cancers. However, imaging is not simply used for detection. Imaging is also important for staging of the disease, determining the precise location of the cancer, helping to guide surgery and other cancer treatments, and checking whether a cancer has returned or not. Molecular imaging is a branch of medical imaging science

that aims to detect, localize, and monitor critical molecular processes in cells, tissues, and living organisms, using highly sensitive instrumentation and contrast mechanisms. This area of medical imaging has developed alongside the emergence of molecular medicine, in which the genetic makeup of each patient is factored into treatment planning. There are many different types of molecular imaging. Amongst them, positron emission tomography (PET) scans may play a role in determining whether or not a mass is cancerous. However, PET scans are more accurate in detecting larger and more aggressive tumors than they are in identifying tumors that are smaller than 8 mm and/or less aggressive. They may also detect cancer when other imaging techniques show normal results. PET scans may be helpful in evaluating and staging recurrent disease. They are beginning to be used to check whether a treatment is working, ie, whether tumor cells are dying and are thus using less sugar.[1–3]

Although conventional treatment options, such as chemotherapy and radiation, have had many advances over the past few decades, cancer therapy is still far from optimal. Its effectiveness depends on a fine balance that is determined by the ability of the therapeutic agent to eradicate the tumor, while affecting as few healthy cells as possible. In this case, the systemic administration of bolus doses of powerful chemotherapeutics often results in intense side effects due to the action of the drugs on sites other than the intended target.[7] With such nonspecific drug action, the concentration of the drug rendered available at the tumor site itself is potentially beneath the minimal effective concentration, putting the patient in the predicament of having to choose between a near-toxic effective dose and a comfortable ineffective dose. In order to alleviate this difficulty, decades of research have focused on developing cancer-specific drugs or delivery systems that can preferentially localize existing agents to the tumor site. Recent advances in nanotechnology promise further developments in target-specific drug delivery systems. Nanoparticles are excellent tumor-targeting vehicles because of the inherent properties of solid tumors.[7] Due to their rapid growth, many solid tumors present with a fenestrated vasculature and poor lymphatic drainage, resulting in an enhanced permeability and retention effect, which allows nanoparticles to accumulate specifically at the tumor site.[4–7]

The 2-fluoro-2-deoxy-D-glucose molecule (^{18}FDG) is a 1.1 nm glucose analog that is most commonly used in PET imaging. The fluorine in the ^{18}FDG molecule is chosen to be the positron-emitting radioactive isotope, ie, fluorine-18, to produce ^{18}FDG. After ^{18}FDG is injected into a patient, a PET scanner can form images of the distribution of ^{18}FDG around the body. The images can be assessed by a nuclear medicine physician or radiologist to diagnose various medical conditions.[1]

As a glucose analog, ^{18}FDG is taken up by cells that use high amounts of glucose, such as the brain, kidney, and cancer cells, where phosphorylation prevents the glucose from being released from the cell after it has been absorbed. The 2'-hydroxyl group in normal glucose is needed for further metabolism of glucose (ie, glycolysis), but ^{18}FDG is missing this 2'-hydroxyl group. Thus, in common with its sister molecule, 2-deoxy-D-glucose, ^{18}FDG cannot be further metabolized in cells. This means that the ^{18}FDG-6-phosphate formed when ^{18}FDG enters the cell cannot move out of the cell before radioactive decay. As a result, the distribution of ^{18}FDG is a good reflection of the distribution of glucose uptake and phosphorylation of cancerous cells in the body.[1,2,7]

As a result, FDG-PET can be used for diagnosis, staging, and monitoring of cancer treatment, particularly in Hodgkin's disease, non-Hodgkin's lymphoma, colorectal cancer, breast cancer, melanoma, and lung cancer.[2] Although tumor metabolic imaging with ^{18}FDG has been studied for more than two decades, the use of this examination in clinical practice is still limited by difficult accessibility, limited availability, and high cost. In addition, PET radiosynthesis must be performed rapidly because of the short half-life of the positron isotopes. Chemical studies of ^{18}FDG are usually complicated and involve long synthesis times (eg, one hour with ^{18}FDG).[3]

With this in mind, Yang et al developed an alternative (^{99m}Tc ethylenedicysteine-deoxyglucose) to ^{18}FDG which has been successfully examined in animal models, and is currently undergoing final multicenter clinical trials where it has also had some success (see Figure 1).[3,4] Even though ^{99m}Tc has some important advantages, such as a longer half-life (six hours), lower costs, and greater availability than ^{18}F, it is also radioactive and consumes charges during the imaging procedure. The chemistry of ^{99m}Tc is also complicated and requires many intermediate conditions, such as the addition and/or adjustment of reducing agents, pH, and coligands.[3]

Magnetic resonance imaging (MRI) is a powerful and noninvasive diagnostic technique based on the differences between the relaxation rates of water protons and it provides important graphic images of the inside of the human body. MRI contrast agents, such as Gd^{3+}-DTPA (gadopentetate dimeglumine, Magnevist®), improve tissue discrimination in MRI images.[5] The most commonly used compounds for contrast enhancement are gadolinium-based. MRI contrast agents alter the relaxation times of tissues and body cavities

where they are present, which, depending on the image weighting, can result in a higher or lower signal.[5]

The main disadvantages of MRI contrast agents are related to lower cellular uptake and nonspecific contrast media targeting. Thus, it would be desirable to develop a simple technique for labeling agents with less expensive paramagnetic metals, such as gadolinium, for tissue-specific targeted imaging, transferring the science of molecular imaging from nuclear medicine to radiological science.

Most MRI contrast agents work by shortening the T1 or T2 relaxation time of protons located nearby. Reduction of the T1 relaxation time results in a hypersignal, whereas a reduced T2 relaxation time reduces both T2 and T2* signals. The effectiveness of the contrast agent depends on its relaxivity (ie, its capacity to modify relaxation times). MRI has the advantage of having a very high spatial resolution and is very adept at morphological and functional imaging. However, MRI does have several disadvantages. First, MRI has a sensitivity of around 10^{-3}–10^{-5} mol/L, which, compared with the other types of imaging, can be very limiting. This problem stems from the fact that the difference between atoms in the high energy state and the low energy state is very small. For example, at 1.5 Tesla, the difference between high and low energy states is approximately nine molecules per two million. Improvements for increasing MRI sensitivity include hyperpolarization, by increasing magnetic field strength, optical pumping, and dynamic nuclear polarization. There are also a variety of signal amplification schemes based on chemical exchanges that increase sensitivity.[3–6]

Furthermore, MRI enables the acquisition of high resolution, three-dimensional images of the distribution of water in vivo. These images are enhanced by the use of contrast agents that catalytically decrease the relaxation time of protons in water in coordination, with a paramagnetic metal center. Gd[III], with seven unpaired electrons and a long electronic relaxation time, is ideally suited for such agents. However, current Gd[III]-based commercial agents have very poor contrast enhancement capabilities due to their low relaxivity. Therefore, these agents are limited to targeting sites where they can be expected to accumulate in high concentrations, such as in the bloodstream and kidneys. The current challenge is to design contrast agents with higher relaxivities that will selectively localize in specific tissues or organs. The most commonly used compounds for contrast enhancement are gadolinium-based.[1–6]

The present paper is the first to describe a new molecular gadolinium-based MRI contrast agent as an alternative to ^{18}FDG that has no radioactive half-life, good availability, reasonable costs, good anticancer effects, with fewer adverse effects on normal human kidneys and powerful precision in MRI oncology and cancer detection at the earliest stages (in brief, a novel bifunctional agent).

Methods

Synthesis

DTPA-dianhydride

The DTPA-dianhydride synthesis procedure has been previously described. Briefly, 7.6 mmol of DTPA 3 g was dissolved in dimethyl sulfoxide 10 mL, acetic anhydride 20 mL, and pyridine 3 mL as a base under anhydrous conditions. The reaction mixture was heated at 65°C for one day. Subsequently, the reaction mixture was cooled, filtered, and washed twice in acetic anhydride and anhydrous diethyl ether. The residue was dried to a constant weight under vacuum (52 kPa) at 40°C, and a white powder was produced with a yield of 93% (see Figure 1).

DTPA-DG

D-glucosamine hydrochloride was neutralized using excess amounts of a base, such as aqueous sodium bicarbonate.[6] The reaction was stirred for at least 30 minutes, then filtered, and ascorbic acid or sodium metabisulphite was added to the solution as an antioxidant agent. The solution was then immediately spray-dried or lyophilized, and a mild yellowish powder (D-glucosamine, base) was obtained, with a yield of 97% (see Figure 1).

DTPA-DA 1 mmol was dissolved in anhydrous diformamide, and then *N,N'*-dicyclohexylcarbodiimide 1.1 mmol, 1-hydroxy-benzotriazole 0.6 mmol, triethylamine 0.2 mL, and activated molecular sieve 3°A 100 mg were added to the medium. The reaction mixture was stirred at room temperature for at least 35 minutes. Afterwards, the reaction temperature was increased to 90–110°C, and D-deoxy-glucosamine (DG) 0.333 mmol was added. The reaction mixture was then heated (90–110°C) for 24 hours. Thin-layer chromatography showed only one spot and no evidence of the starting material. The reaction mixture was then cooled at room temperature (25 ± 1°C), diluted with water 0.2 mL and methanol 5 mL, and then filtered. A clear solution was collected, and diethyl ether was added one drop at a time to the solution until a white DTPA-monoamide (DTPA-DG) crystallized. This was then filtered. The above steps were repeated for further purification until a yellowish-orange powder was obtained. Alternatively, DTPA-DG was obtained from the refluxation of toluene/activated molecular sieve 3°A and glucosamine at temperatures over 90°C.

The DTPA-DG was purified using a dialysis bag with a cutoff point of 500 Da in water (green chemistry) for a period of 24 hours. The remaining solution was removed from the dialysis bag and then lyophilized. A pure white powder was obtained with an overall yield of 40%. When ultrasonication was used, an overall yield of 71% was obtained.

Preparation of GDD

One mmol of DTPA-DG was reacted in water with 1 mmol of $GdCl_3$ at room temperature for at least 30 minutes. The reaction mixture was then dialyzed using a dialysis bag (cutoff point 100–500 Da) and lyophilized. The yellowish crystalline powder was identified by ultraviolet spectroscopy as Gd^{3+}-DTPA-DG (GDD). The ability of DTPA-DG to form a complex with Gd^3 is illustrated in supplementary Figure 1.

T1/T2 measurement

The T1- and T2-weighted spin echo images at 1.5 Tesla (repetition time/echo time 250/16 msec and repetition time/echo time 4000/64 msec) were analyzed qualitatively. The signal intensities of vials with contrast medium in solution and contrast medium in cells with the corresponding iron concentrations were visually compared. For quantitative data analysis, the MRI images obtained were transferred as DICOM images to Dicom (digital imaging and communication in medicine) Works Software (v 1.3.5),[7,8] and, for each concentration, three samplings and the maximum regions of interest were considered. Five concentrations of GDD (0.33, 0.17, 0.08, 0.04, and 0.02 mmol/mL) were obtained by dilution with sodium chloride 0.9% (Figure 2).

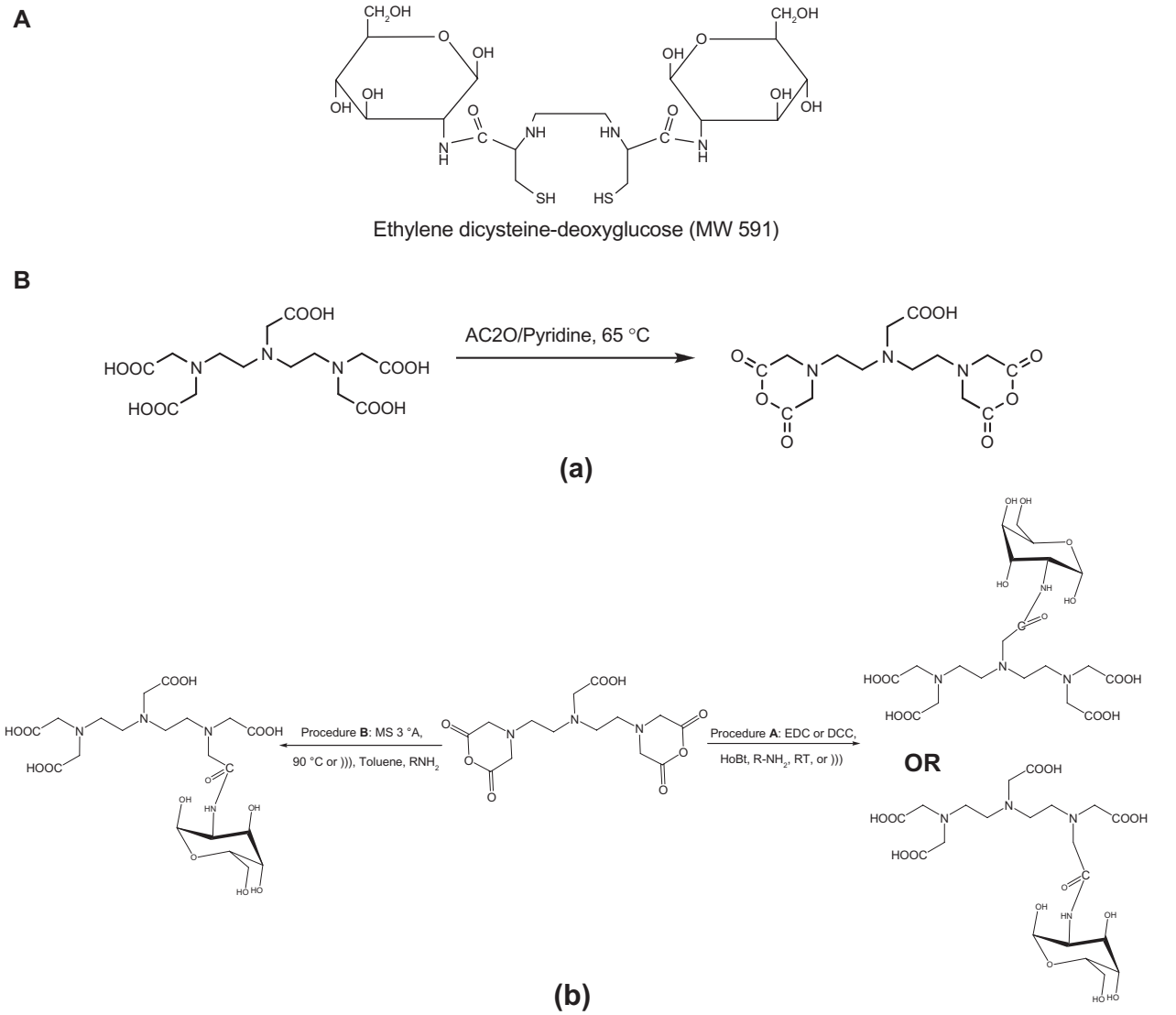

Figure 1 A) Chemical structure of ethylenedicysteine deoxyglucose. **B**) General procedure for synthesis of (**a**) DTPA-DA and (**b**) DTPA-DG.
Abbreviations: DTPA, diethylenetriamine penta-acetic acid-D-glucosamine; DTPA-DG, diethylenetriamine penta-acetic acid-D-deoxy-glucosamine.

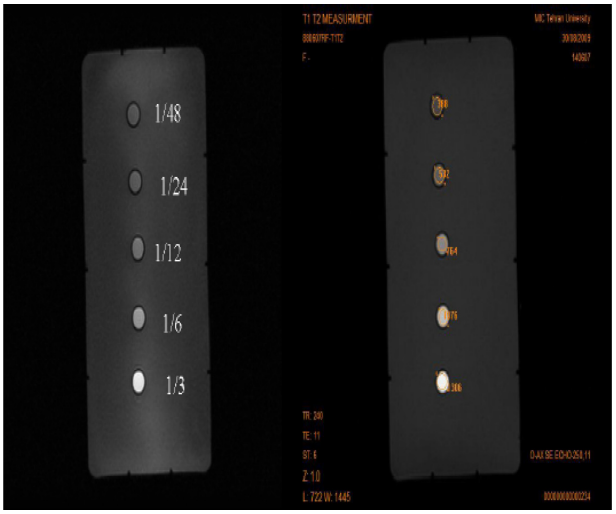

Figure 2 Schematic illustration of performance of in vitro T1/T2 measurements using magnetic resonance imaging apparatus. For each concentration, triplicate sampling and the maximum region of interest were considered. Five concentrations of Gd^{3+}-DTPA-DG (0.33, 0.17, 0.08, 0.04, and 0.02 mmol/mL) were obtained by dilution with sodium chloride 0.9%.
Abbreviation: Gd^{3+}-DTPA-DG, gadopentetate dimeglumine-D-deoxy-glucosamine.

All imaging protocols were performed on a 1.5 T GE MRI (Sigma, St Louis, MO) system. Relaxation rates of gadolinium-loaded complex contrast agents were measured at different concentrations, using different spin echo and gradient echo protocols. For T2 measurement, two multiecho spin echo protocols were used, with echo times of 12, 24, 36, and 48 msec and of 46, 92, 138, and 184 msec (repetition time 1000 msec, Equation 1):

$$Signal_{SE} = S_0 e^{-R_2 \cdot TE} \quad (1)$$

Repetition time-variable spin echo imaging (with the same echo time values) was used for T1 measurement. For T2 measurement, multiecho spin echo protocols were used, with repetition times of 60, 140, 240, 340, 440, 600, 800, 1000, 1500, 2000, 3000, and 5000 msec (echo time 11 msec).

The signal intensity equation used for T1 measurement is shown in Equation 2.

$$Signal_{SE} = S_0 (1 - e^{-TR/T_1}) \quad (2)$$

The T1 and T2 maps were calculated assuming Môn exponential signal decay. The T1 maps were calculated from four spin echo images, with a fixed echo time of 11 msec at 1.5 Tesla and variable repetition times of 60, 140, 240, 340, 440, 600, 800, 1000, 1500, 2000, 3000, and 5000 msec, using a nonlinear function least-square curve fitted on a pixel-by-pixel basis. The signal intensity for each pixel as a function of time was expressed as follows:

Slpixel xy (t) = So(pixel xy) (1–exp (–t/T1 pixel xy)).

The T2 maps were calculated accordingly from four spin echo images with a fixed repetition time of 1000 msec and echo time values of 12, 24, 36, and 48 msec. The signal intensity for each pixel as a function of time was expressed as follows:

Slpixel xy (t) = So(pixel xy) exp (–t/T2 pixel xy).

Care was taken to analyze only data points with signal intensities significantly above the noise level. The T1 and T2 relaxation times (s) of the samples in the Eppendorf tubes were derived by region of interest measurements of the test samples on these T1 and T2 maps, and the results were converted to R1 and R2 relaxation rates (s–1).

For this purpose, five nude mice (mean weight 18 ± 1.2 g) bearing the human lung cancer cell line were used. T1 and T2 relaxation times were obtained using multipoint techniques, including repetition time points of 400–3000 msec, with a constant echo time of 12 msec for T1 measurement and echo time points under 48 msec, with a constant repetition time of 2000 msec for T2 measurement, respectively. Coronal spin echo images (for T1 and T2 relaxation times) were obtained with a slice thickness of 2.5 mm and a 0.2 mm gap, a 256 × 256 matrix size, a 12 × 12 field of view, a 31.2 kHz bandwidth, and two averages in order to reach an appropriate resolution and signal to noise ratio.

Stability test

The GDD was dissolved in water and added to a solution containing 0.1 N ethylenediamine tetra-acetic acid in phosphate buffer and gently stirred for at least 24 hours. The mixture was then dialyzed, and the T1/T2 of the remaining solution was measured.

In vitro cell toxicity

Human fibrosarcoma epithelial-like (HT1080), human colon adenocarcinoma Grade II (HT29), human non-small cell lung cancer, human kidney proximal tubular (HKC-5) and human embryonic kidney 293 (HEK 293) cell lines were obtained from the Iran Pasteur Institute and used for cell cytotoxicity and inflammation response studies. The cells were grown in 25 cm^2 culture flasks using complete RPMI-1640. The cell culture medium was supplemented with 10% fetal bovine serum and 1% penicillin-streptomycin at 37°C with 5% CO_2 in an incubator. The cells were subcultured every 72 hours and harvested from subconfluent cultures (70% using 0.05% trypsin-ethylenediamine tetra-acetic acid). The cells were cultured at 10^4 cells/well in 96-well plates in all of the experiments, except for the apoptosis-necrosis and tumor necrosis

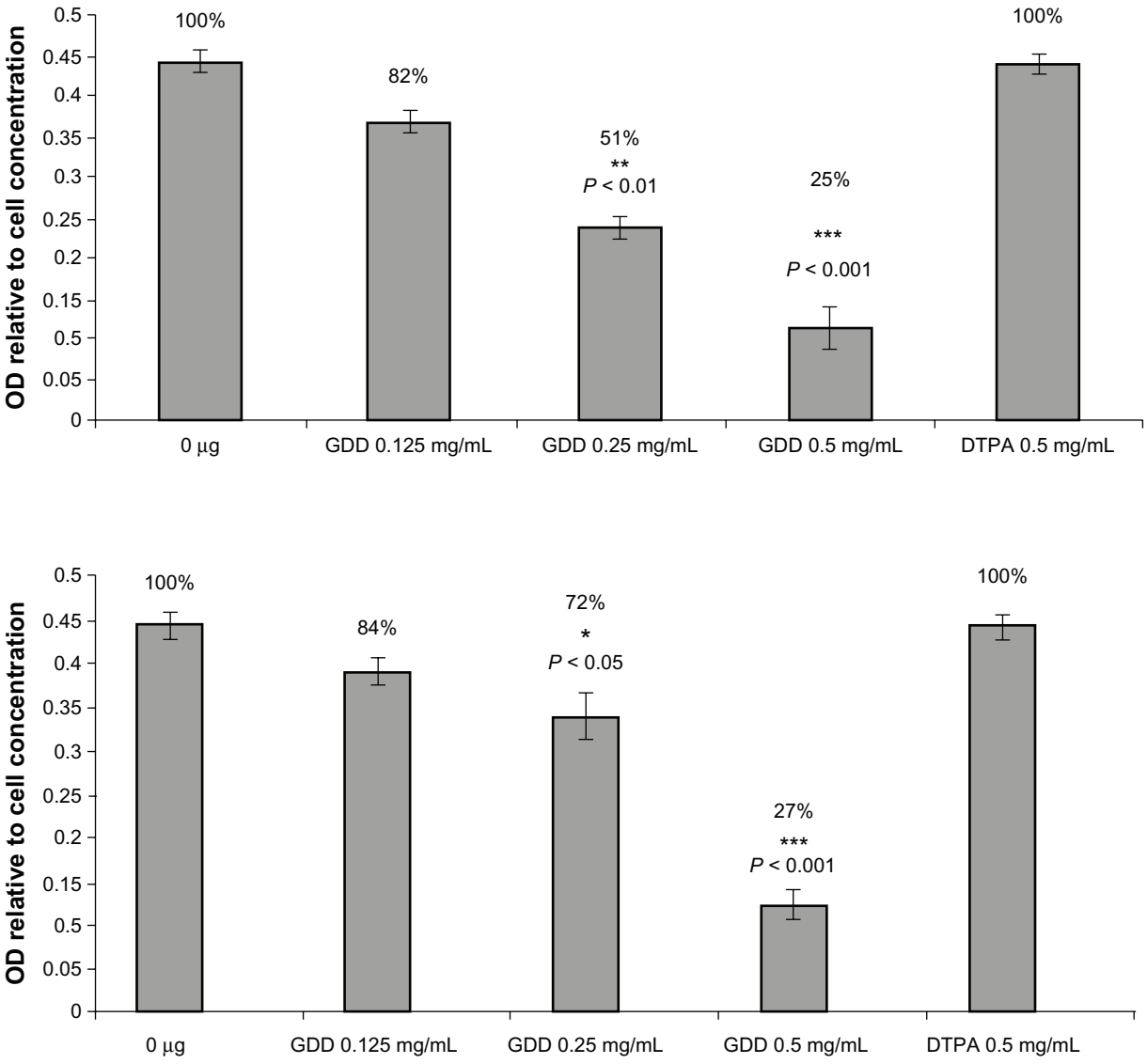

Figure 3A MTT results of 48 hours of Gd^{3+}-DTPA-DG exposure to HT1080 and HT29 cell lines. The average percent of viable cells is also shown.
Abbreviation: Gd^{3+}-DTPA-DG, gadopentetate dimeglumine-D-deoxy-glucosamine.

factor alpha (TNF-α) secretion assays, in which 12-well plates at 10^6 cells/mL were used.

MTT assay

The MTT assay is a technique used widely for cell viability measurements,[9] and is based on the reduction of MTT to formazan by viable cells. At the end of the incubation periods (24 and 48 hours), the supernatant of the HT1080 cells was removed, MTT solution was added to each well of the plates at a final concentration of 0.5 mg/mL GDD, and the cells were incubated for an additional four hours. Thereafter, the solution was removed, the cells were lysed, and the dye was dissolved in 100 µL dimethyl sulfoxide. The plates were kept in the dark for one hour in order to be ready for spectrophotometric determination. The amount of absorption in each well, reflecting the conversion of MTT to formazan by the metabolically viable cells, was calculated using an automated microplate reader at 570 nm. The results were compared with untreated control cultures. The same procedures were performed on two human kidney cell lines (incubated with concentrations of 0.125, 0.25, and 0.5 mg/mL GDD).

TNF-α assay

To determine if complex causes of cell death were involved in the initial mechanism, the amount of TNF-α secretion was analyzed using a U-CyTech^R enzyme-linked immunosorbent assay kit. After 24 hours of GDD incubation at a final concentration of 0.5 mg/mL with the HT1080

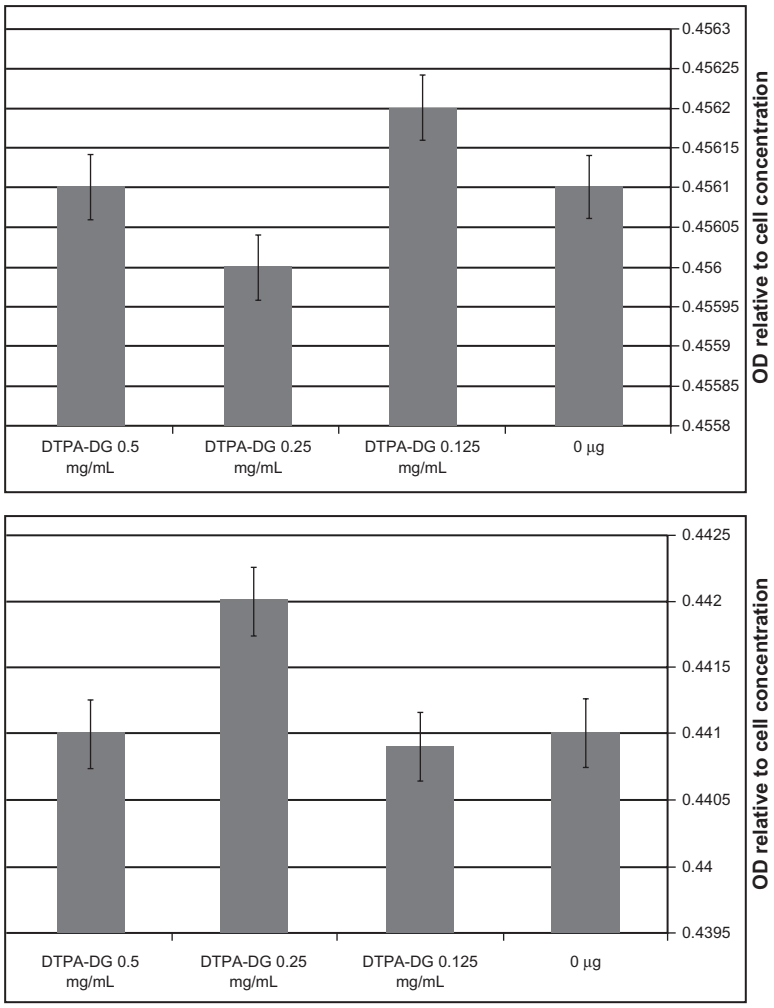

Figure 3B MTT results of 48 hours of Gd^{3+}-DTPA-DG exposure to HKC-5 and HEK-293 human kidney cell lines. No significant toxic effect was observed.
Abbreviation: Gd^{3+}-DTPA-DG, gadopentetate dimeglumine-D-deoxy-glucosamine.

cell line, the cells were pelleted, and the supernatants collected and used for quantitative determination of TNF-α secretion according to a specific protocol at 450 nm with a microplate reader. The negative control only contained complete RPMI-1640.[10]

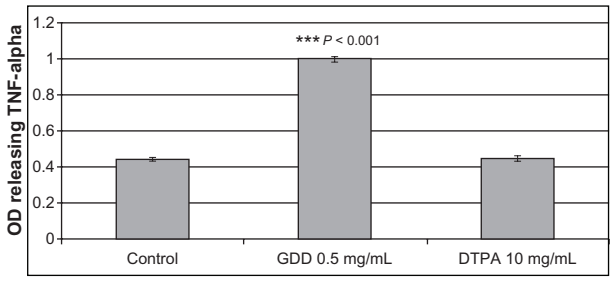

Figure 4 Effect of Gd^{3+}-DTPA-DG and DTPA on TNF-α release. As depicted, the complex increased TNF-α release significantly.
Abbreviations: DTPA, diethylenetriamine penta-acetic acid; Gd^{3+}-DTPA-DG, gadopentetate dimeglumine-D-deoxy-glucosamine.

Prothrombin time-activated partial thromboplastin time coagulation assay

Different concentrations of the complex were tested for their impact on coagulation processes. The prothrombin time test was used to investigate the extrinsic and common coagulation pathways. The activated partial thromboplastin time assay was used to assess intrinsic and common coagulation pathways. In order to perform the experiments, different concentrations of the complex solutions in phosphate-buffered saline were incubated for five minutes before adding the kit reagents. Once the tissue thromboplastin was added to the anticoagulated blood samples, the times required for the formation of fibrin clots were measured by visual inspection.[10] The study results were expressed in seconds and compared with the negative controls which only contained phosphate-buffered saline (1:9; ie, the ratio of complex solution to the blood sample).

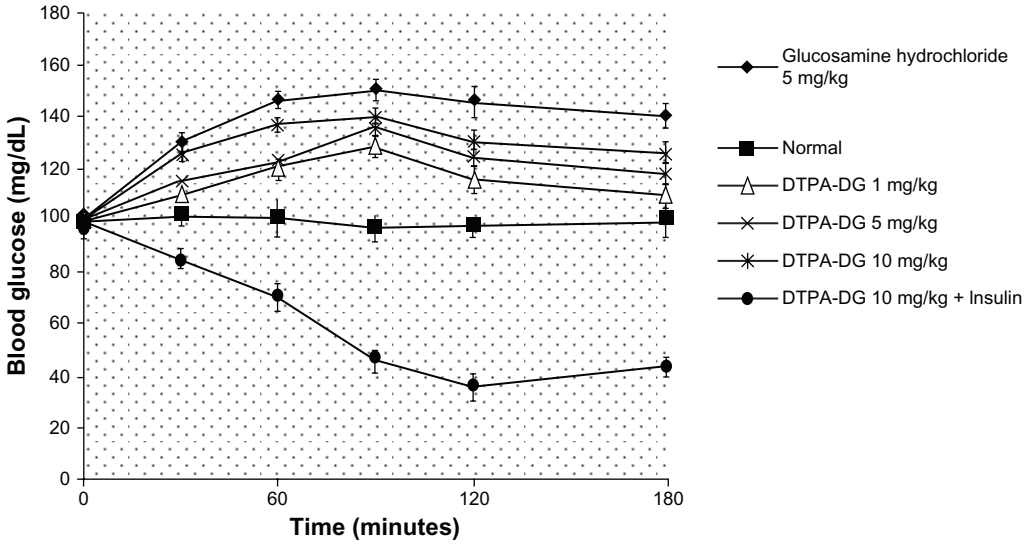

Figure 5 Effect of DTPA-DG on blood glucose level in rats. No significant changes were observed.
Abbreviation: DTPA-DG, diethylenetriamine penta-acetic acid-D-deoxy-glucosamine.

Blood sample preparation

Anticoagulated blood samples (3.2% sodium citrate) were obtained from healthy, nonmedicated volunteers. Platelet-poor plasma was isolated by centrifuging the whole blood at 3000 rpm for 15 minutes at room temperature. The blood samples were used as prepared.

Labeled gadolinium-loaded glucose at different concentrations was tested for its impact on the coagulation process. Prothrombin time was used to investigate the extrinsic and common coagulation pathway, while the activated partial thromboplastin time assay was used to assess the intrinsic and common coagulation pathway. In order to perform these experiments, the complex solutions were incubated for five minutes in phosphate-buffered saline at different concentrations before adding the kit reagents. After tissue thromboplastin was added to the anticoagulated blood samples, the time required for forming a fibrin clot was measured by visual inspection.[11] The results were expressed in seconds and compared with the control, which only contained phosphate-buffered saline (1:9; ie, the ratio of complex solution to the blood sample).

Table 1A Positive hexokinase enzyme response to Gd^{3+}-DTPA-DG, glucose, and glucosamine

Glycosylated compounds at same concentrations	Hexokinase activation after three minutes of incubation (340 nm)
Glucose	+
Glucosamine	+
Gd^{3+}-DTPA-DG	+

Abbreviation: Gd^{3+}-DTPA-DG, gadopentetate dimeglumine-D-deoxy-glucosamine.

Microscopic observations

To determine if complex causes of cell death were involved in the initial morphological changes after 24 hours of incubation of the HT1080 cell line with GDD, changes in cell morphology were observed using an inverse phase-contrast microscope (Wilovert®, Hund Wetzlar, Wetzlar, Germany) and DTPA, DTPA-DG, and Magnevist® were studied in the control groups.

Hexokinase assay

A hexokinase assay was performed to determine whether GDD mimics glucose phosphorylation or not. Using a ready-made assay kit (Sigma), GDD 3.44 mg, glucose 1 mg, and DG 1 mg were separately dissolved in 1 mL of water. Next, 200 µL was removed from each of the four solutions and diluted in 2.5 mL of water. A 10 µL aliquot of each solution was removed, mixed with 900 µL of Infinity™ glucose reagent (Sigma), and then incubated at 37°C for three minutes. The reduced form of nicotinamide adenine dinucleotide resulting from glucose phosphorylation showed absorption at 340 nm.[3]

Blood glucose level alterations

Various doses of DTPA-DG were intravenously injected into rats (six rats per group), and changes in the blood glucose level were determined and compared with those in the control groups, including insulin (glucose-lowering agent [negative control]), glucosamine (glucose-increasing agent [positive control]), and normal (the group that did not receive any compound),[3] because when presenting a glucose moiety

Table 1B T1 values (msec) derived from equations 1 and 2

TR	Concentration					Water
	1/3	1/6	1/12	1/24	1/48	
60	551	358	260	206	186	116
140	1035	729	468	330	251	156
240	1385	1076	764	532	394	259
340	1542	1292	971	694	520	350
440	1628	1458	1133	835	635	434
600	1705	1581	1317	1005	794	559
800	1756	1667	1478	1197	956	692
1000	1767	1684	1544	1304	1070	793
2000	1800	1767	1739	1649	1488	1212
T1	161.2643122	253.421186	420.3446826	666.2225183	916.5902841	1367.427868
1/T1	0.006201	0.003946	0.002379	0.001501	0.001091	0.0007313
R^2 value	0.99	0.99	0.9875	0.9964	0.9971	0.9973

structure in the complex it seems necessary to measure the changes in blood glucose by DTPA-DG.

Animals

Throughout the experiment, the nude mice were kept in $16 \times 28 \times 13$ cm plastic cages and the rats in stainless steel cages, three to six in each, maintained in a conventional animal room at the Pasteur Institute of Iran, which was air-conditioned (21–22°C and 60%–70% relative humidity) and ventilated 16 times/hour, and provided with an adequate diet and tap water ad libitum. The animal experiments were carried out in accordance with the recommendations of the Declaration of Helsinki and the internationally accepted principles for use of experimental animals, and they were also confirmed by the local ethics committee of our institution.

Cancer animal model

Each animal was xenografted in the right foreleg muscle with 4×10^6 human non-small cell lung cancer cells. Two weeks after grafting, the tumors had attained a size of about 4 mm in diameter.

MRI tumor imaging studies

The tumor-bearing animals (each group, n = 3, mean weight 18 ± 1.3 g) were anesthetized with ketamine 50 mg/kg and xylazine 5 mg/kg, 0.1 mM each of GDD and Gd^{3+}-DTPA (which was determined in the T1/T2 relaxivity test) was injected into the mice, and they were then placed in the clinical MRI apparatus (1.5 Tesla, GE Sigma). The T1-weighted MRI procedures were performed prior to and 25 minutes after injection.

MRI brain studies

In order to investigate whether or not the experimental complex mimicked ^{18}FDG brain pharmacokinetics, the above mentioned imaging procedures were performed 20 minutes after intravenous injection for brain imaging and compared with the Gd^{3+}-DTPA control group (Magnevist®).

Results and discussion

Size and zeta potential distribution

As can be seen in supplementary Figure 2, when the gadolinium-loaded conjugate was formed from the DTPA-DG

Table 1C T2 values (msec) derived from equations 1 and 2

TE	Concentration					Water
	1/3	1/6	1/12	1/24	1/48	
10	1762	1602	1340	1022	800	546
25	1372	1263	1097	862	711	478
40	1200	1172	1044	835	697	463
55	1043	1018	943	775	653	456
70	962	920	911	762	641	445
1/T2	0.0099	0.00883	0.00615	0.00462	0.00352	0.00305
T2	101.010101	113.25028	162.601626	216.450216	284.09	327.87
R^2 value	0.96	0.97	0.92	0.88	0.91	0.8

Table 1D The average corresponding Magnevist® T1 values as comparison standard

Magnevist 1.5 mM	T1 relaxation time
1/3	178
1/6	280
1/12	433
1/24	678
1/48	924
Water	1363

and Gd^{3+}, we observed a negative charge and a size of approximately 8 nm at a concentration of 0.02 mg/mL. This may have resulted from the more negative groups being available at its surface. These phenomena could result from the crosslinking of nitrogen and oxygen atoms with the gadolinium ion, which intercalates between three nitrogens of the conjugate molecule and also masks the negative charges (due to carboxylate ions) of the DTPA for the reaction with gadolinium.

MTT assay

The MTT test was performed on two cancer cell types, HT1080 and HT29, and also on the two human kidney cell lines, HEK 293 and HKC-5. The 24-hour exposure of GDD did not show any significant toxicity on these cell types, but continued exposure for 48 hours showed very significant ($P < 0.05$) and powerful anticancer potency for GDD (Figure 3A). It should also be noted that the complex at these concentrations did not show any toxic effects on normal human kidney cells (Figure 3B). The unlabeled ligands (DTPA and DTPA-DG) were also demonstrated to be safe.

TNF-α assay

To investigate the initially hypothesized mechanism of the observed anticancer effect of GDD, a TNF-α assay was performed. GDD caused a significant ($P < 0.05$) increase in TNF-α release (Figure 4). This indicates the possibility of inflammation mediating the observed cell death as a potential initial mechanism.

Table 1E Mean Gd^{3+}-DTPA-DG T1 values (msec) from stability testing. Each sample was repeated at least three times

Gd^{3+}-DTPA-DG concentration	T1 relaxation time
1/3	175
1/6	275
1/12	429
1/24	677
1/48	922
Water	1363

Abbreviation: Gd^{3+}-DTPA-DG, gadopentetate dimeglumine-D-deoxy-glucosamine.

Blood glucose levels

A nonsignificant ($P > 0.05$) increase in blood glucose levels was observed after intravenous injections of DTPA-DG at various doses. The coadministration of DTPA-DG and insulin caused a marked decrease in blood glucose levels. This illustrates the effectiveness of insulin on cell/tissue uptake of DTPA-DG (Figure 5).

Hexokinase assay

Absorption at 340 nm for GDD, DTPA-DG, D-glucose, and DG (Table 1A) was a sign of glucose phosphorylation due to the presence of the reduced form of nicotinamide adenine dinucleotide.

Prothrombin and activated partial thromboplastin times

It has been thought that GDD can have effects on blood calcium and cause coagulation disorders, but the results of these experiments showed no significant effects (Figure 6).

Morphological changes

The number of HT1080 cancer cells was significantly reduced only by GDD (Figure 7) after 48 hours of exposure to the experimental complex. As qualitative evidence, in addition to the aforementioned results, the complex caused cell death by activation of TNF-α, although more details of this need to be investigated in future experiments.

T1/T2 measurement

T1 relaxivity was 62.5 mM^{-1} s^{-1} and T2 relaxivity was 24.4 mM^{-1} s^{-1} at 37°C and 1.5 Tesla in sodium chloride 0.9% and the r2:r1 ratio was 2.56. An important aspect of GDD is the low concentration required (compared with the 0.5 mM concentration required for Magnevist) and achieving appropriate relaxivity. This is an additional benefit of the gadolinium-loaded complex.

The T1/T2 relaxation time results (calculated from equations 1 and 2) are shown in Tables 1B and 1C and Figures 8A and 8B (the spin echo and gradient echo protocol results needed to be further processed to derive the data in Tables 1B and 1C). GDD caused a significant ($P < 0.001$) decrease in both T1 and T2 relaxation times compared with Magnevist (Table 1D) and water.

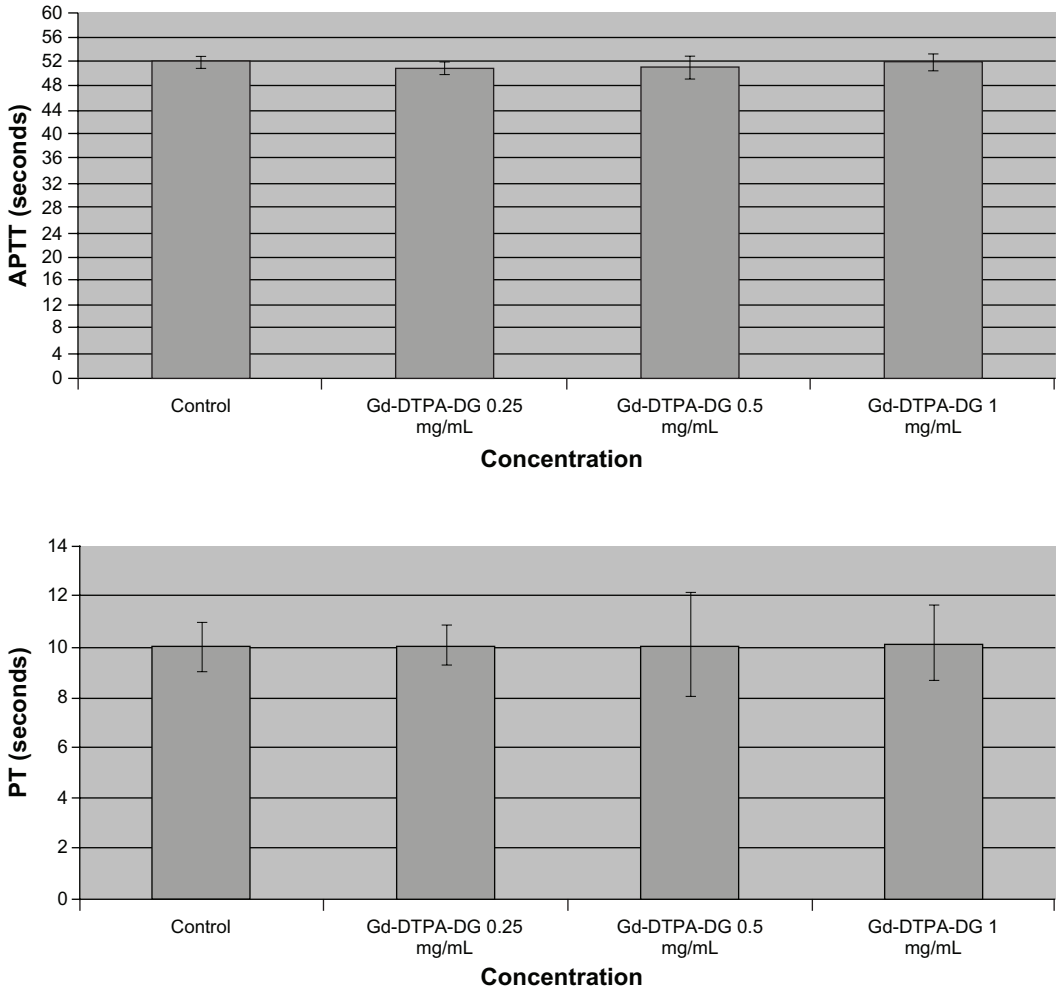

Figure 6 Effects of the experimental complex on coagulation factors. No significant changes were observed in PT and APTT factors.
Abbreviations: PT, prothrombin time; APTT, activated partial thromboplastin time.

The corresponding mean data for heart and brain tumor location in vivo T1/T2 relaxation time measurements 10 and 20 minutes after injection of Magnevist and GDD are shown in Table 2.

Stability test

No significant observations were found before or after exposure of GDD to the ethylenediamine tetra-acetic acid solution (Table 1E).

MRI studies

Tumor areas were found 20 minutes after GDD injection (an average of three mice was used for each image, see Figures 9A and 9B). The tumor location in the MRI images (T1-weighted method) 20 minutes after intravenous GDD injection in the mice bearing the human lung cancer cell line was enhanced. The MRI images (T1-weighted method) 20 minutes after intravenous Gd^{3+}-DTPA (Magnevist + GDD [Figures 9A and 9C] and Gd^{3+}-DTPA [Figures 9A–9D]) injection in mice bearing the human lung cancer cell line were also obtained. As predicted, Magnevist was not capable of enhancing tumor location significantly, but due to angiogenesis in the cancer cells, some enhancement as a result of Magnevist accumulation was observed, and an increase in MRI visibility was observed on coadministration of both contrast agents (Figures 9A–9C).

The hearts of the mice were observed after GDD injection, as shown in Figure 10. The gastrointestinal tract was also clearly enhanced when compared with controls. Additionally, significant enhancement of the MRI brain images was also obtained for GDD injection compared with Magnevist, the latter showing no enhancement, and this provides clear neurological evidence that the pharmacokinetics of the complex mimic those of ^{18}FDG (Figure 10).

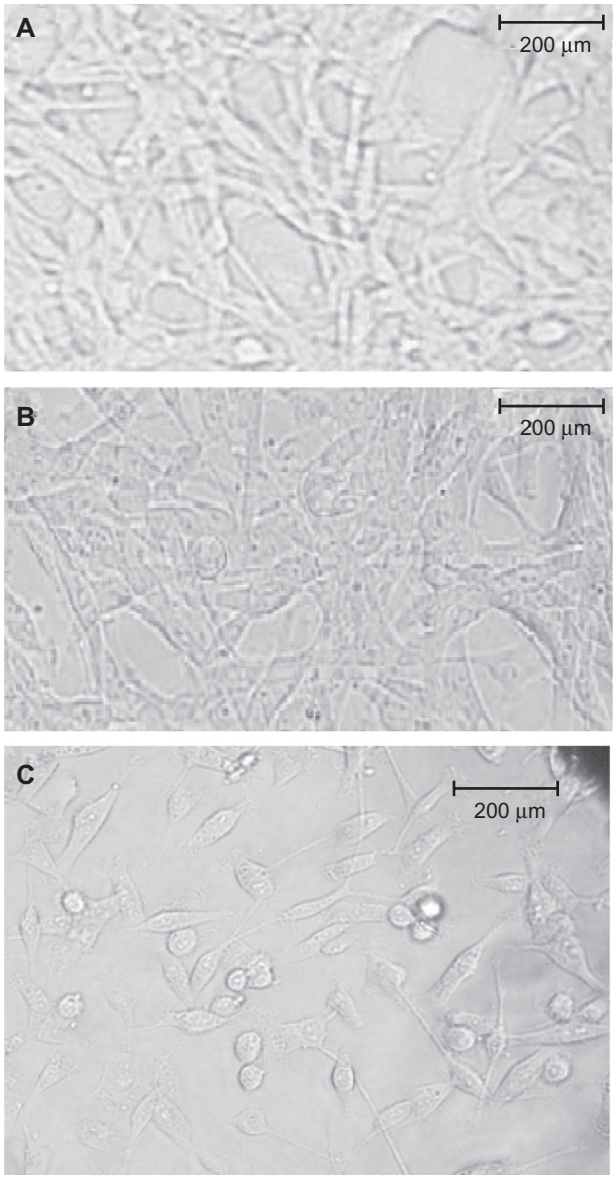

Figure 7 Morphological changes in HT1080 cells. **A**) Control group without any treatment, **B**) 0.125 mg/mL Gd^{3+}-DTPA-DG, and **C**) 0.5 mg/mL Gd^{3+}-DTPA-DG. The amount of HT1080 cancer cells was observed to diminish significantly only in the Gd^{3+}-DTPA-DG group.
Abbreviation: Gd^{3+}-DTPA-DG, gadopentetate dimeglumine-D-deoxy-glucosamine.

As reported in the literature, ^{18}FDG was distributed throughout three major parts of the body, ie, heart, tumor, and brain, and therefore its major applications would be in cardiology, oncology, and neurology.[1,2] As a result, it is assumed that GDD mimics the pharmacokinetics of ^{18}FDG very closely.

The results show that the GDD conjugate highlighted tumor areas in an animal model of human lung cancer. Moreover, anticancer activity, phosphorylation by the hexokinase enzyme, and no significant alterations in blood glucose levels or coagulation factors, were also found for this complex. Furthermore, increased TNF-α release and a good lowering of T1/T2 potency was found. MRI contrast agents, such as Gd^{3+}-DTPA, improve tissue discrimination in the MRI images.[5,12]

The findings indicate the potential possibilities of the GDD complex being used as an alternative to ^{18}FDG in the near future. The gadolinium-loaded complex was phosphorylated by the hexokinase enzyme and was proven to have similar cell entrance mechanisms and metabolism as ^{18}FDG. DTPA is classified as an extracellular fluid contrast agent because of its reduced uptake by cells, and this is the main disadvantage of the compound.[12,13] To increase cellular uptake of DTPA (as a potential Gd^{3+} chelator), especially in cancer cells, a well recognized glucose conjugation strategy[14] was employed in this study.

When DG is conjugated to DTPA, the resulting compound has the ability to enter cells and may be used to treat intracellular radiometal overload or, in the context of radiopharmaceutical labeling or MRI, has the ability to penetrate cancer cells. For example, the GDD complex may be used as a novel selective strategy in oncology for the diagnosis and/or treatment of tumors, thus confirming our hypothesis. Moreover, ^{18}FDG and glucosamine have structural similarities in that they have a fluorine atom and an amino group at position 2 of the glucose moiety. DTPA-DG also has an amino group at this position in its glucose moiety.[3,4]

The molecular structure of glucosamine has several structural features, including amino, acetyl, and carboxyl groups at key positions that, on mediation by N-acetylglucosamine transferase in the nucleolemma, facilitate its entry into tumor cell nuclei, reflecting tumor cell proliferation. In summary, glucosamine is a highly attractive scaffold for a glucosyl ligand because the amine acts both as a potential coordination site and as a useful target for further functionalization. Furthermore, there is much evidence in the literature to suggest that N-functionalized glucosamines show activity with glucose transporters and hexokinase enzymes that are most closely associated with the metabolism of ^{18}FDG, even when the functional group is large.[15,16]

Finally, it should be noted that the amino-conjugating region of DTPA is not important, and the only important factor is DTPA-DG production. Hence, the difference in the DTPA region of conjugation to the amino compound does not produce any complications in its application, such as metal-complex formation or cell uptake.[6] On the other hand, the binding site of the targeted amino compound is very important, eg, in the case of DG, where the binding sites are limited to carbon numbers 1 and 2 because other

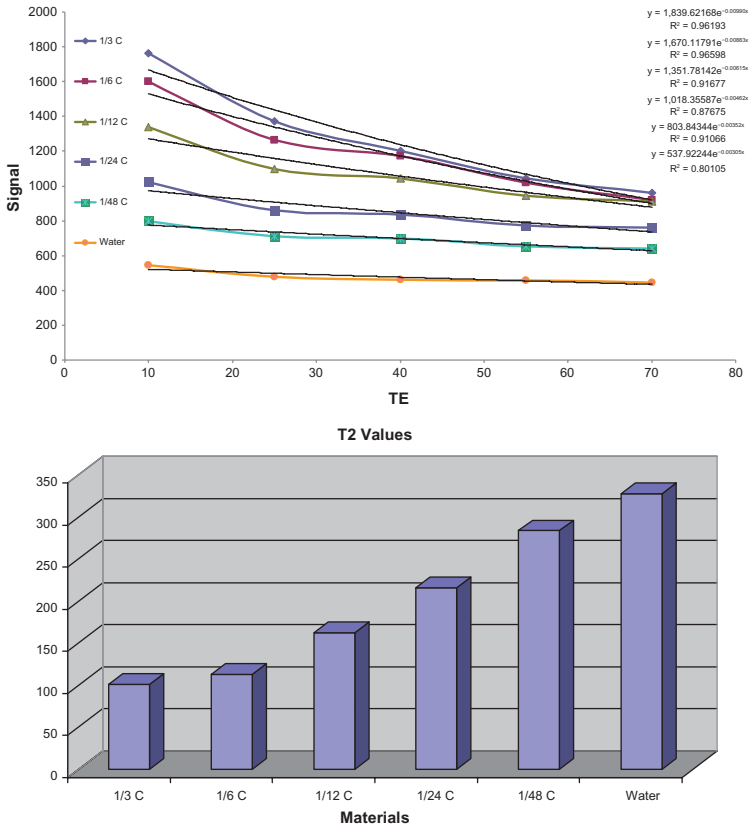

Figure 8A T2 data based on spin echo and gradient echo protocols.

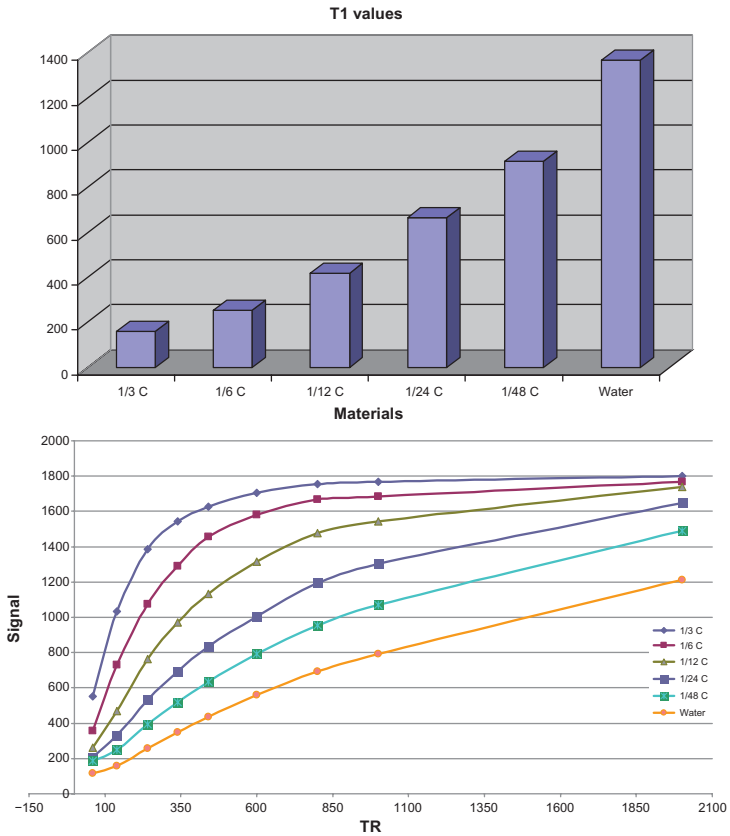

Figure 8B T1 data based on spin echo and gradient echo protocols.

Table 2 Mean in vivo T1, T2 data for Gd^{3+}-DTPA-DG and Magnevist® relaxation times at different time points and tissues are shown as the mean ± standard error of the mean for tumor-bearing nude mice (mean weight 18 ± 1.3 g, n = 3 in each group)

Tissue	Brain [Gd^{3+}-DTPA-DG]	Heart [Gd^{3+}-DTPA-DG]	Tumor [Gd^{3+}-DTPA-DG]	Brain [Magnevist]	Heart [Magnevist]	Tumor [Magnevist]
T1 (10 minutes)	365 ± 7	155 ± 9	145 ± 5	1333 ± 10	1123 ± 12	543 ± 8
T1 (20 minutes)	191 ± 4	87 ± 8	118 ± 8	1321 ± 11	1167 ± 10	442 ± 9
T2 (10 minutes)	189 ± 6	98 ± 10	102 ± 9	1002 ± 12	876 ± 13	398 ± 11
T2 (20 minutes)	101 ± 9	45 ± 7	89 ± 8	999 ± 14	882 ± 11	298 ± 7

Notes: *Decimal values are not shown; **Square brackets indicate concentrations.
Abbreviation: Gd^{3+}-DTPA-DG, gadopentetate dimeglumine-D-deoxy-glucosamine.

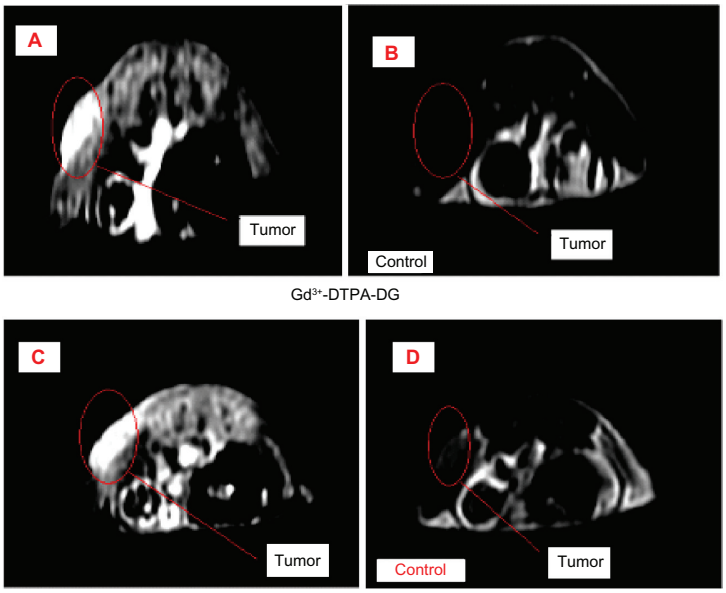

Figure 9A Magnetic resonance images (T1 weighted method) prior and 20 minutes after Gd^{3+}-DTPA-DG intravenous injection (**A** and **B**) in mice bearing human lung cancer (each image was performed on three mice). The tumor site was definitely enhanced. Magnetic resonance images (T1 weighted method) 20 minutes post Gd^{3+}-DTPA + Gd^{3+}-DTPA-DG (**C**) and Gd^{3+}-DTPA (Magnevist®, **D**) intravenous injection in mice bearing human lung cancer.
Abbreviations: Gd^{3+}-DTPA-DG, gadopentetate dimeglumine-D-deoxy-glucosamine; Gd^{3+}-DTPA, gadopentetate dimeglumine.

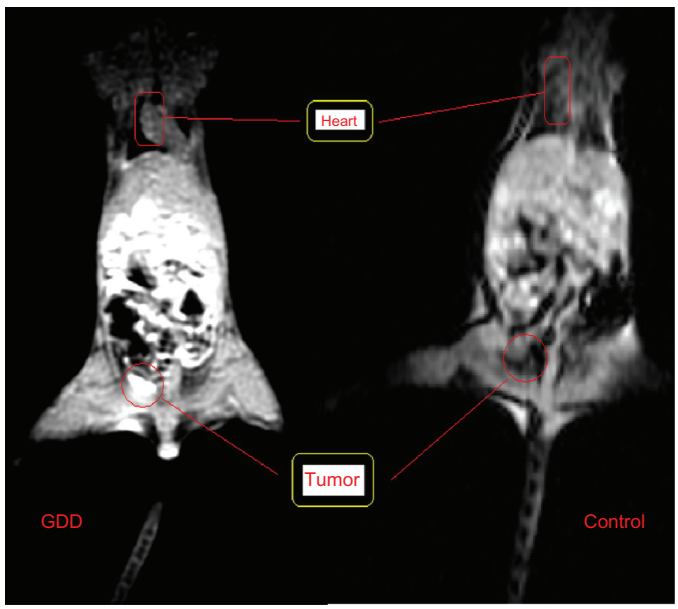

Figure 9B Illustration of the whole body magnetic resonance images prior and 20 minutes post intravenous Gd^{3+}-DTPA-DG injection in mice bearing human lung cancer cells.
Abbreviation: Gd^{3+}-DTPA-DG, gadopentetate dimeglumine-D-deoxy-glucosamine.

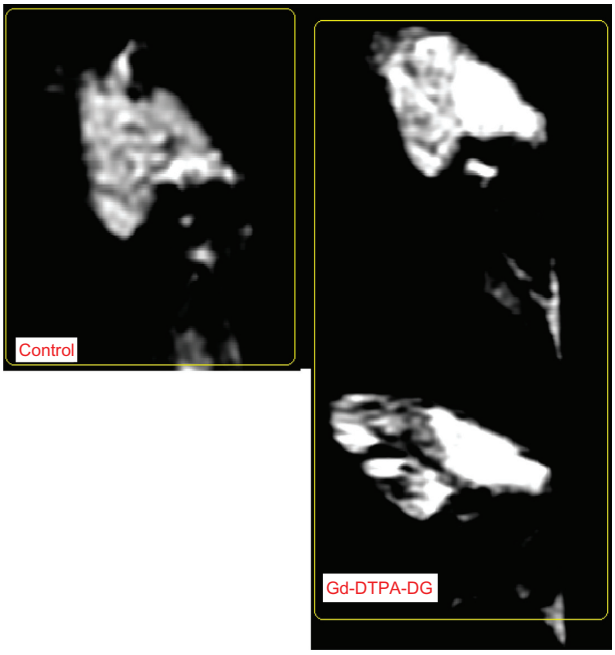

Figure 10 Illustration of the ability of Gd^{3+}-DTPA-DG to penetrate the blood-brain barrier. The nude mice brain was significantly enhanced 20 min post intravenous Gd^{3+}-DTPA-DG injection. As observed, Magnevist® could not enhance the animal brain resolution. Gd^{3+}-DTPA-DG seems to show the same pharmacokinetics as ^{18}FDG in the brain as well as in the gastrointestinal tract and tumor sites.
Abbreviation: Gd^{3+}-DTPA-DG, gadopentetate dimeglumine-D-deoxy-glucosamine.

carbons have an important role in cell uptake, and the metabolism of hexose and conjugation at these sites may produce complications.[17]

Also, a nanosized GDD conjugate could decrease T1/T2 relaxation times to a significantly greater extent than Magnevist. Another interesting aspect of this research concerns the toxic effect of the experimental complex on cancerous cell lines but without toxic effects on normal kidney cell lines at the same concentrations.

Adverse events following intravenous injection of gadolinium contrast media are less common than for iodinated agents, and are estimated to occur in less than 5% of patients. However, acute renal failure, ie, a sudden and rapid deterioration in renal function causing failure to excrete nitrogenous waste products or to maintain fluid and electrolyte homeostasis, may occur as a result of intravascular administration of radiographic and MRI contrast media.[18–20]

Conclusion

Contrast medium-induced nephropathy ranges in severity from asymptomatic, nonoliguric transient renal dysfunction to severe acute oliguric renal failure necessitating dialysis. Serum creatinine often peaks within three to four days after the administration of contrast media.[18] Fortunately, most episodes of contrast medium-induced nephropathy are self-limiting and resolve within one to two weeks. Patients with contrast medium-induced nephropathy have a higher mortality rate (31%) than patients without contrast medium-induced nephropathy (0.6%) after primary angioplasty for acute myocardial infarction.[18] These side effects are often caused by free gadolinium uptake by kidney cells resulting from instability of the gadolinium complex in vivo.[18] No significant toxicity and/or complex instability in vitro was observed for human kidney cell lines, and these are further important advantages of nanosized GDD.

There are similarities between the uptake of GDD and that of ^{18}FDG in tumors, and our findings support the potential use of nanosized GDD conjugates as functional metabolic MRI agents. In addition, DTPA-DG can be easily and efficiently labeled with gadolinium, in a stable and cost-effective manner. Given the complex mechanisms expressed in tumor tissue growth, this method of investigation has the potential to improve the diagnosis, prognosis, and planning and monitoring of cancer treatment.

This complex was generated and examined for the first time as a new MRI agent. Future experiments, eg, investigation of caspase activation to determine the anticancer effect of the complex-induced cytotoxicity in cancerous cell lines to prove the concept of inflammation mediators or ^{18}FDG comparative imaging, are needed to determine the value of this newly proposed alternative to ^{18}FDG.

Acknowledgment

This paper is a major part of a registered PhD dissertation in radiopharmacy, and was supported by the Tehran University of Medical Sciences. The authors would like to express their deep gratitude to all technicians who provided support in any form during the course of this research.

Disclosure

This paper was presented at the 26th Iranian Congress of Radiology held on May 13–16, 2010, in Tehran, and has been published in abstract form.[21] Otherwise, the authors report no conflicts of interest in this work.

References

1. Cheze-Le Rest C, Metges JP, Teyton P, et al. Prognostic value of initial fluorodeoxyglucose-PET in esophageal cancer: a prospective study. *Nucl Med Commun*. 2008;29:628–635.
2. Parente P, Coli A, Massi G, et al. Immunohistochemical expression of the glucose transporters Glut-1 and Glut-3 in human malignant melanomas and benign melanocytic lesions. *J Exp Clin Cancer Res*. 2008;27:34–40.
3. Yang DJ, Kim CG, Schechter NR, et al. Imaging with 99 mTc ECDG targeted at the multifunctional glucose transport system: Feasibility study with rodents. *Radiology*. 2003;226:465–473.

4. Schechter NR, Erwin WD, Yang DJ, et al. Radiation dosimetry and biodistribution of [99 m]Tc ethylenedicysteine-deoxyglucose in patients with non-small-cell lung cancer. *Eur J Nucl Med Mol Imaging*. 2009; 36:1583–1591.
5. Geraldes CF, Laurent S. Classification and basic properties of contrast agents for magnetic resonance imaging. *Contrast Media Mol Imaging*. 2009;4:1–23.
6. Shafiee-Ardestani M, Jabbari-Arabzadeh A, Heidari Z, et al. Novel and facile methods for the synthesis of DTPA-mono-amide; a new completely revised strategy in radiopharmaceutical chemistry. *J Radioanal Nucl Chem*. 2010;283:447–455.
7. Puech PA, Boussel L, Belfkih S, Lemaitre L, Douek P, Beuscart R. DicomWorks: Software for reviewing DICOM studies and promoting low-cost teleradiology. *J Digit Imaging*. 2007;20:122–130.
8. Vlerken LEV, Amiji MM. Multi-functional polymeric nanoparticles for tumour-targeted drug delivery. *Expert Opin Drug Deliv*. 2006;3: 205–216.
9. Puech P, Boussel L. DicomWorks 1.3.5. Available at: http://www.dicomworks.com. Accessed May 22, 2006.
10. Mosmann T. Rapid colorimetric assay for cellular growth and survival: Application for proliferation and cytotoxicity assay. *J Immunol Methods*. 1983;65:55–63.
11. Motlagh D, Yang J, Lui KY, Webb AR, Amee GA. Hemocompatibility evaluation of poly [glycerol-sebacate] in vitro for vascular tissue engineering. *Biomaterials*. 2007;27:4315–4324.
12. Haririan I, Shafiee-Alavidjeh M, Khorramizadeh MR, Shafiee-Ardestani M, Zarei-Ghane Z, Namazi H. Anionic linear-globular dendrimer-cis-platinum [II] conjugates promote cytotoxicity in vitro against different cancer cell lines. *Int J Nanomedicine*. 2010;5:63–75.
13. Kainthan RK, Hester SR, Levin E, Devive DV, Brooks DE. In vitro biological evaluation of high molecular weight hyperbranched polyglycerols. *Biomaterials*. 2007;28:4581–4590.
14. Werner EJ, Botta M, Aime S, Raymond KN. Effect of a mesitylene-based ligand cap on the relaxometric properties of Gd[III] hydroxypyridonate MRI contrast agents. *Contrast Media Mol Imaging*. 2009;4: 220–229.
15. Raymond KN, Pierre VC. Next generation, high relaxivity gadolinium MRI agents. *Bioconjug Chem*. 2005;16:3–8.
16. Sun YY, Chen Y. Cancer drug development using glucose metabolism radiopharmaceuticals. *Curr Pharm Des*. 2009;15:983–987.
17. Marshall S, Nadeau O, Yamasaki K. Glucosamine-induced activation of glycogen biosynthesis in isolated adipocytes: Evidence for a rapid allosteric control mechanism within the hexosamine biosynthesis pathway. *J Biol Chem*. 2005;280:110–118.
18. Black AR, Black JD, Azizkhan-Clifford J. Sp1 and kruppel-like factor family of transcription factors in cell growth regulation and cancer. *J Cell Physiol*. 2001;188:143–151.
19. Schibli R, Dumas C, Petrig J, et al. Synthesis and in vitro characterization of organometallic rhenium and technetium glucose complexes against glut 1 and hexokinase. *Bioconjug Chem*. 2005;16:105–112.
20. Baert AL, Sartor K, editors. *Medical Radiology Diagnostic Imaging*. Heidelberg, Germany: Springer; 2006.
21. Ardestani MS. Potential Opponent for 18FDG: Gd3+-DTPA-DG: A New Synthetic MRI Contrast Agent. *Iranian J Radiol*. 2010;7 (Suppl 1):56.

Supplementary materials

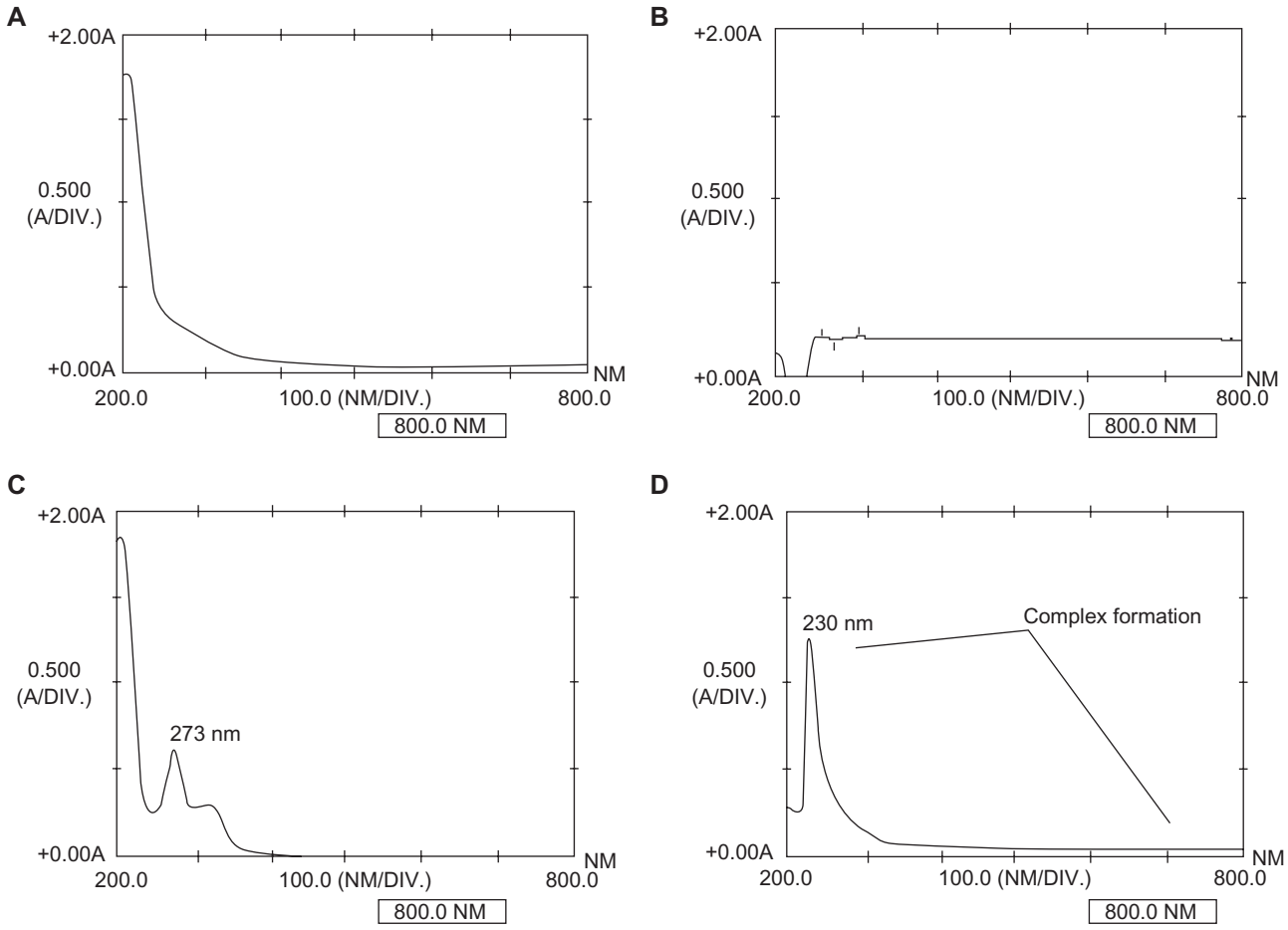

Figure S1 Illustration of the original U.V spectrums of DTPA (**A**), D-Glucosamine (**B**), DTPA-DG (**C**), and Gd^{3+}-DTPA-DG (**D**).

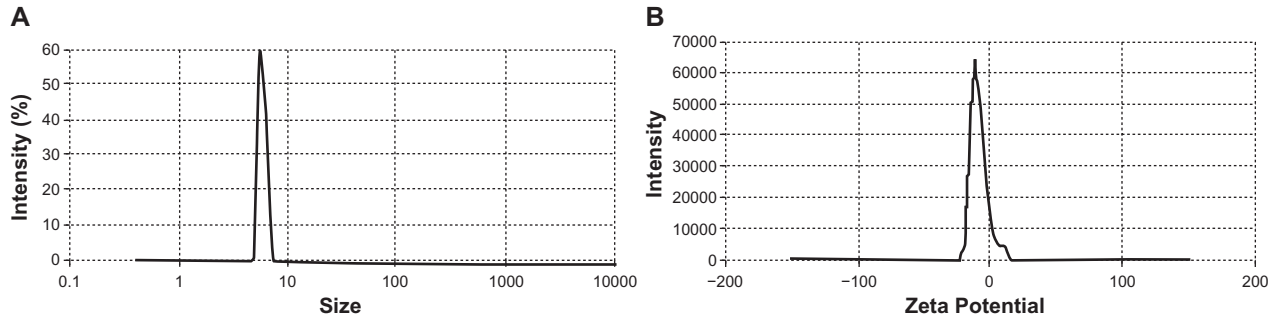

Figure S2 Size and zeta potential distribution. **A**) size and **B**) zeta potential distribution of the DTPA-DG compound according to concentration.